THE JOURNAL OF BIOLOGICAL CHEMISTRY VOL. 287, NO. 29, pp. 24585–24594, July 13, 2012

Spatial Coordination of Kindlin-2 with Talin Head Domain in Interaction with Integrin β Cytoplasmic Tails*

Received for publication, December 21, 2011, and in revised form, May 29, 2012 Published, JBC Papers in Press, May 30, 2012, DOI 10.1074/jbc.M111.336743

Kamila Bledzka[‡], Jianmin Liu[‡], Zhen Xu[§], H. Dhanuja Perera[‡], Satya P. Yadav[¶], Katarzyna Bialkowska[‡], Jun Qin[‡], Yan-Qing Ma[§1], and Edward F. Plow[‡2]

From the [‡]Department of Molecular Cardiology, Joseph J. Jacobs Center for Thrombosis and Vascular Biology/NB-50 and [¶]Research Core Services, Department of Molecular Biotechnology, Lerner Research Institute, Cleveland Clinic, Cleveland, Ohio 44195 and [§]Blood Research Institute, Blood Center of Wisconsin, Milwaukee, Wisconsin 53226

Background: The talin and kindlin play indispensable roles in integrin activation.
Results: The C-terminal 12 amino acids of β_1 and β_3 integrins mediate kindlin-2 binding.
Conclusion: Kindlin-2 binding to the extreme C terminus allows β subunits to accommodate both kindlin-2 and talin.
Significance: Binding of talin and kindlin-2 to distinct sites in integrins regulates receptor activation, a pivotal event in cellular responses.

Both talin head domain and kindlin-2 interact with integrin β cytoplasmic tails, and they function in concert to induce integrin activation. Binding of talin head domain to β cytoplasmic tails has been characterized extensively, but information on the interaction of kindin-2 with this integrin segment is limited. In this study, we systematically examine the interactions of kindlin-2 with integrin β tails. Kindlin-2 interacted well with β_1 and β_3 tails but poorly with the β_2 cytoplasmic tail. This binding selectivity was determined by the non-conserved residues, primarily the three amino acids at the extreme C terminus of the β_3 tail, and the sequence in β_2 was non-permissive. The region at the C termini of integrin β_1 and β_3 tails recognized by kindlin-2 was a binding core of 12 amino acids. Kindlin-2 and talin head do not interact with one another but can bind simultaneously to the integrin β_3 tail without enhancing or inhibiting the interaction of the other binding partner. Kindlin-2 itself failed to directly unclasp integrin α/β tail complex, indicating that kindlin-2 must cooperate with talin to support the integrin activation mechanism.

Activation of integrins is a key mechanism to control many cellular adhesive responses including platelet aggregation, leukocyte trafficking, and endothelial cell migration (1, 2). At a molecular level, the integrin activation process is controlled tightly by the heterodimeric α/β cytoplasmic tail (CT)[3] complex formed between the membrane-proximal regions of each integrin subunit, and this complex extends into their transmembrane domains (3, 4). The α/β CT complex restrains the integrin in a resting, low affinity state for extracellular ligands, and a process to unclasp the complex is required to initiate integrin activation (5).

Mechanistically, integrin activation is balanced by multiple CT-associating proteins, including both activators and inhibitors, and the coordination of these positive and negative regulators, together with post-translational modifications of the β CT, defines the clasping state of integrin CT, and thereby integrin activation (6–11). Among many integrin CT binding proteins, the head domain of the cytoskeletal protein talin (talin-H) is a well characterized integrin activator (12, 13). Talin-H resides at the N terminus of talin and resembles a FERM domain, which contains four subdomains (F_0, F_1, F_2, and F_3). The integrin binding sites in talin is auto-inhibited but can be exposed by calpain cleavage or binding partners, which allows its F3-phosphotyrosine binding subdomain to directly interact with integrin β CT and unclasp the CT complex to induce integrin activation (14–21). However, quantitative analysis indicated that talin-H alone is insufficient to induce efficient integrin activation, and a co-activation model was proposed (6, 22). Within recent years, it has been found that kindlins could dramatically enhance talin-mediated integrin activation in model cells and were also essential to support efficient integrin activation *in vivo*, verifying a co-activation mechanism (23–25). Indeed, deficiencies of specific kindlins are associated with diseases in human, which reflect an inability to effectively activate integrins (26–29). The kindlin family contains three members in mammals, and among them, kindlin-2 is expressed ubiquitously and enriched in the integrin-containing adhesion complexes (30, 31). Interestingly, kindlin family members also contain a FERM-like domain, which is preceded by a distinct F_0 subdomain at the N terminus and with a pleckstrin homology domain inserted in the middle of its F_2 subdomain, both of which are potential binding sites for membrane phosphoinositides (32–34) While sharing a structurally similar FERM domains, mutations in the integrin β CTs have distinct effects on kindlin and talin-H binding (23–25, 35, 36).

* This work was supported, in whole or in part, by National Institutes of Health Grants P01HL073311 and R01 HL096062 from the NHLBI. This work was also supported by Scientist Development Grant 10SDG2610277 and a postdoctoral fellowship (Great Rivers Affiliate POST4310067) from the American Heart Association.

[1] To whom correspondence may be addressed: Blood Research Institute, Blood Center of Wisconsin, 8727 Watertown Plank Rd., Milwaukee, WI 53226. E-mail: yanqing.ma@bcw.edu.
[2] To whom correspondence may be addressed: Dept. of Molecular Cardiology/NB-50, 9500 Euclid Ave., Cleveland, OH 44195. E-mail: plowe@ccf.org.

[3] The abbreviations used are: CT, cytoplasmic tail; EGFP, enhanced GFP; SPR, surface plasmon resonance; HSQC, heteronuclear single quantum coherence; FERM, 4.1 protein ezrin radixin moesin.

To further understand the regulatory role of kindlin in integrin activation, we have measured the interaction of kindlin-2 to integrin and detected an unexpected binding preference for different integrin β CTs. Further detailed mapping using synthesized peptides defined a 12-amino acid kindlin-2 binding core in the C termini of integrin β CT. Residues at the extreme C terminus of this binding core establish the preference of kindlin-2 for different integrin β CTs. Kindlin-2 alone could not unclasp the integrin CT complex, demonstrating that kindlin-2 is dependent upon talin-H to support integrin activation. Finally, despite the relatively large size of kindlin-2 and talin-H, we demonstrate that the short integrin β CTs can accommodate both co-activators simultaneously to achieve integrin co-activation, a transition that governs many cellular responses, including platelet aggregation inflammatory cell recruitment and tumor metastasis (37–39).

EXPERIMENTAL PROCEDURES

Protein Preparation and Peptide Synthesis—GST-fused integrin β CT, full-length kindlin-2 and His-tagged talin-H(1–429) were expressed, purified, and quantified as described previously (10). Talin-F_2F_3(206–405) was prepared as described previously (40). All synthetic peptides were prepared, purified, and authenticated by HPLC and MALDI TOF-TOF (matrix-assisted laser desorption ionization time-of-flight) mass spectrometry in the Molecular Biotechnology Core of the Cleveland Clinic.

Pulldown Assays and Western Blotting—Pulldown assays were performed using GST fusion proteins. Equal amounts of GST-fused integrin β CTs were added together with glutathione-Sepharose 4B (GE Healthcare) to aliquots of the cell lysates from either EGFP-kindlin-2-expressing CHO cells or HUVECs. In peptide inhibition experiments, the indicated peptide was added to the slurries at the selected concentrations. After overnight incubation in a cold room, the precipitates were washed and boiled in Laemmli sample buffer. The eluates were analyzed on gradient acrylamide gels under reducing conditions, and interactions of the integrin β CT with kindlin-2 were determined by Western blotting. The gels were also stained with Coomassie blue to verify that sample loadings were similar.

Surface Plasmon Resonance (SPR)—Real time protein-protein interactions were analyzed using a Biacore3000 instrument (Biacore, Uppsala, Sweden). Purified proteins were immobilized on the carboxymethyl dextran of CM5 biosensor chip using the standard amine coupling chemistry, and biotinylated peptides were captured on a SA sensor chip (Biacore) according to the manufacturer's instructions. Experiments were performed at room temperature in 10 mM HEPES (pH 7.4) buffer containing 150 mM NaCl and 0.005% surfactant P20 at a flow rate of 25 μl/min. SPR sensograms were obtained by injecting various concentrations of analyte. The chip surfaces were regenerated by injecting a short pulse of 5 mM NaOH. The resulting sensograms were analyzed in overlay plots using BIAevaluation software (version 4.01, GE Healthcare). The association (k_a), dissociation (k_d) rates constant and the affinity constant (K_A and K_D) were calculated by global fitting (1:1 Langmuir model).

Isothermal Titration Calorimetry—Purified talin-H and kindlin-2 proteins were dialyzed into 50 mM phosphate buffer (pH 8.0). Talin-H at the concentration of 1.4 mM was titrated into the solution of kindlin-2 at a 70 μM concentration in a Microcal iTC200 instrument (GE Healthcare). Isothermal titration calorimetry titration curves were obtained by tirating talin-H in 10 3-μl injections with 70 μM kindlin-2 solution in the cell. Titration curves were collected to estimate heat changes associated with the kindlin-2/talin-H interaction.

NMR Spectroscopy—Two-dimensional transferred NOESY experiments were performed with mixing time of 400 ms on Bruker Avance 600 MHz at 25 °C as described (16). The spectra were processed and visualized using nmrPipe (41). Two-dimensional HSQC experiments used to examine the integrin β CT-target binding were described previously (16).

Cell Spreading—To test the function of the kindlin-2 binding core in a cellular system, a series of chimeric PSGL-1/β3 constructs were expressed in $\alpha_{IIb}\beta_3$-CHO cells, and their effects of cell spreading were assessed. The chimera consisted of the extracellular and transmembrane domains of PSGL-1 (mPSGL-1) fused to selected segments of the β_3CT. This approach, described previously (23), allows expression of functional segments or mutants of the β_3CT in the cytosol while tethered to PSGL-1, which allows for monitoring of expression levels. The specific chimeric proteins were β_3CT/PSGL-1 (β_3(468–762)), β_3CTΔ748/PSGL-1 β_3(468–748), β_3CT-(CORE)/PSGL-1 (β_3CTΔ716+749–762), and these were transfected into $\alpha_{IIb}\beta_3$-CHO cells. In short, the transiently transfected cells were allowed to adhere and spread on fibrinogen-coated (20 μg/ml) glass coverslips. After incubation at 37 °C for 2 h, the wells were washed three times with PBS, and the adherent cells were fixed with 4% paraformaldehyde and stained with Alexa Fluor 647 phalloidin (Invitrogen). To identify PSGL-1-expressing cells, the fixed cells were stained by anti-PSGL-1 mAb, KPL-1 (BD Biosciences), followed by goat anti-mouse IgG conjugated with Alexa Fluor 488 (Invitrogen). As controls, nontransfected cells were included in each experiment and always showed no PSGL-1 staining. The positively stained (green) cells were visualized with a ×40 oil immersion objective using a Leica TCS-NT laser scanning confocal microscope (Imaging Core, Cleveland Clinic). Cell area was analyzed with ImageJ software.

Statistical Analysis—Two-tailed Student's *t* tests were performed using SigmaPlot (version 11). Differences were considered to be significant with $p < 0.05$.

RESULTS

Kindlin-2 Exhibits Selective Binding to Integrin β Cytoplasmic Tails—Previous studies have demonstrated that the ability of kindlin-2 to bind and activate β_1 and β_3 integrins depends on its interaction with the membrane-distal N*xx*Y motif in the β subunit of these integrins (23–25). Because the membrane distal N*xx*Y/F motif is conserved across different integrin β subunits (Fig. 1*A*), we postulated that kindlin-2 might bind to other integrin β CTs similarly. Surprisingly, we failed to detect interaction of expressed kindlin-2 in cell lysates with GST-fused integrin β_2 CT in pulldown assays (Fig. 1*B*). As expected, kindlin-2 could be precipitated by integrin β_1 or β_3 CTs under the

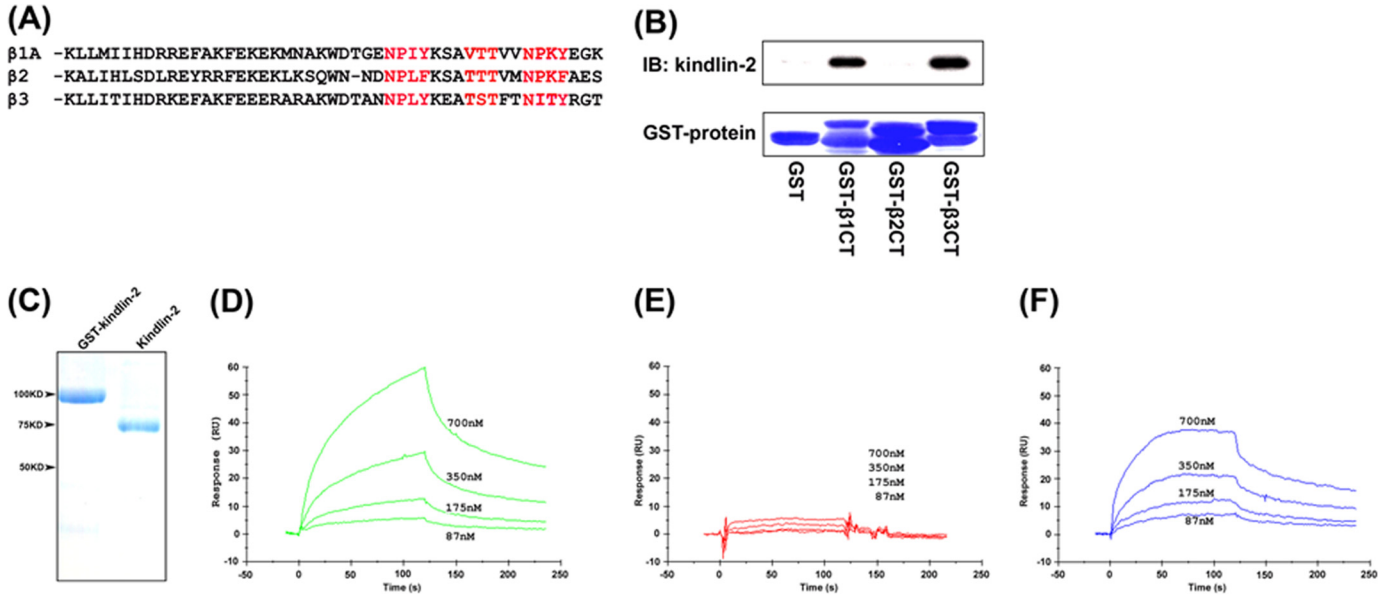

FIGURE 1. **Kindlin-2 binds to the integrin β CT.** *A*, alignment of the amino acids sequences of the β_1, β_2, and β_3 cytoplasmic domains, in which two N*xx*Y motifs and S/T cluster implicated in kindlin-2 binding are highlighted in *red*. *B*, GST or GST-fused β CT were incubated with the lysates of EGFP-kindlin-2-transfected CHO cells together with glutathione-Sepharose. After washing, the bound kindlin-2 was analyzed by SDS-PAGE and Western blot with anti-EGFP antibody. Coomassie Blue staining was used to verify similar loading of the GST proteins onto the gels. *C*, SDS-PAGE of the purified kindlin-2 protein with GST and after GST cleavage. The full-length CTs of β_1 (*D*), β_2 (*E*), and β_3 (*F*) were immobilized on the CM5 sensor chip surfaces (~400 RU), respectively. Various concentrations of kindlin-2 protein were injected over the coated chips, and the progress curves of binding were recorded on a Biacore3000 instrument. *IB*, immunoblot.

same condition. The sequence of all three β CTs, including the β_2 CT, was confirmed, and this preference in kindlin-2 binding was observed with multiple preparations of the β_2 CT. To verify these results, we measured the direct binding of purified kindlin-2 protein to integrin β CTs. Kindlin-2 was expressed as a GST fusion protein in *Escherichia coli* and purified as described previously (Fig. 1*C*) (10). Real time binding of kindlin-2 to full-length integrin β CTs was monitored by SPR in which kindlin-2 protein was injected and allowed to flow over immobilized full-length β_1, β_2, or β_3 CT. As shown in Fig. 1, *D* and *F*, kindlin-2 bound to the β_1 and β_3 CTs. Consistent with the pulldown results, only minimal binding of kindlin-2 to immobilized β_2 CT was detected (Fig. 1*E*). The dissociation constants for kindlin-2 with the full-length β_1 and β_3 CTs were similar at 1.77×10^{-7} and 1.36×10^{-7} M, respectively. Based on the concentrations used, we estimated that the affinity of kindlin-2 for the β_2 CT was at least 100-fold lower than for the β_1 or β_3 CT. These results suggest that kindlin-2 can interact selectively with different integrin β CTs and indicate that the conserved motifs in the integrin β CTs are insufficient to determine kindlin-2 recognition.

Identification of Kindlin-2-binding Site in Integrin β Cytoplasmic Tails—We previously implicated residues in the C-terminal region of the integrin β_1 and β_3 CTs in kindlin-2 binding (Fig. 2*A*) (10, 23). To more precisely define the requirements for their interaction, we directly immobilized these β C-terminal peptides conjugated with biotin at their N termini onto SA biosensor chips for SPR analysis. As shown in Fig. 2*B*, kindlin-2 bound to the immobilized β_1 and β_3 C-terminal peptides, but the association with the β_2 C-terminal peptide was significantly lower, confirming the interactive selectivity of kindlin-2 to integrin β CT. The similar kindlin-2 dissociation constants for the C-terminal peptides and their full-length versions (1.77×10^{-7} M for full-length β_1 and 1.96×10^{-7} M for the β_1 C-terminal peptide; 1.36×10^{-7} M for full-length β_3 CT and 1.81×10^{-7} M for the β_3 C-terminal peptide) verified that the C termini of the integrin β_1 and β_3 CT served as the main binding region for kindlin-2.

To further define the kindlin-2-binding site, a series of peptides corresponding to the C termini of the β_1 CT with sequential deletion of residues from both the C- and N-terminal sides were synthesized. The β_1 peptides synthesized are shown in Fig. 2*C*, and they were tested as inhibitors of the β_3-GST/kindlin-2 co-precipitation. As shown in Fig. 2*C*, the β_1 CT peptides containing the highlighted residues (AVTTVVNPKYEG, designated as the β_1 core) were effective blockers of kindlin-2 binding to the β_3 CT, whereas the β_1 CT peptides lacking these highlighted residues were ineffective inhibitors. The counterpart peptide of β_3 CT (ATSTFTNITYRG, designated as β_3 core) also effectively blocked kindlin-2 binding to the β_1 or β_3 CT, as did the β_1 core (Fig. 2, *D* and *E*). Thus, the 12 amino acid residues in the β CTs identified in Fig. 2*A* constitute the basic binding core for kindlin-2 recognition with high affinity.

Intriguingly, the kindlin-2 binding core in the integrin β CTs contains both conserved and variable residues (Figs. 1*A* and 2*A*). To further test the contribution of these non-conserved residues in the integrin β CTs for kindlin-2 interaction, we generated chimeric β peptides in which the last three variable residues in the β_2 and β_3 CTs were replaced with each other (Fig. 2*F*). By SPR analysis, we found substitution of the last three residues RGT in the β_3 peptide with the β_2 counterpart residues AES nearly abolished the interaction of β_3 CT peptide with kindlin-2. Surprisingly, replacement of AES in the β_2 CT peptide with RGT significantly enhanced kindlin-2 binding to the β_2 CT peptide (Fig. 2*G*). These results demonstrate that the variable residues in integrin β CTs also contribute to kindlin-2

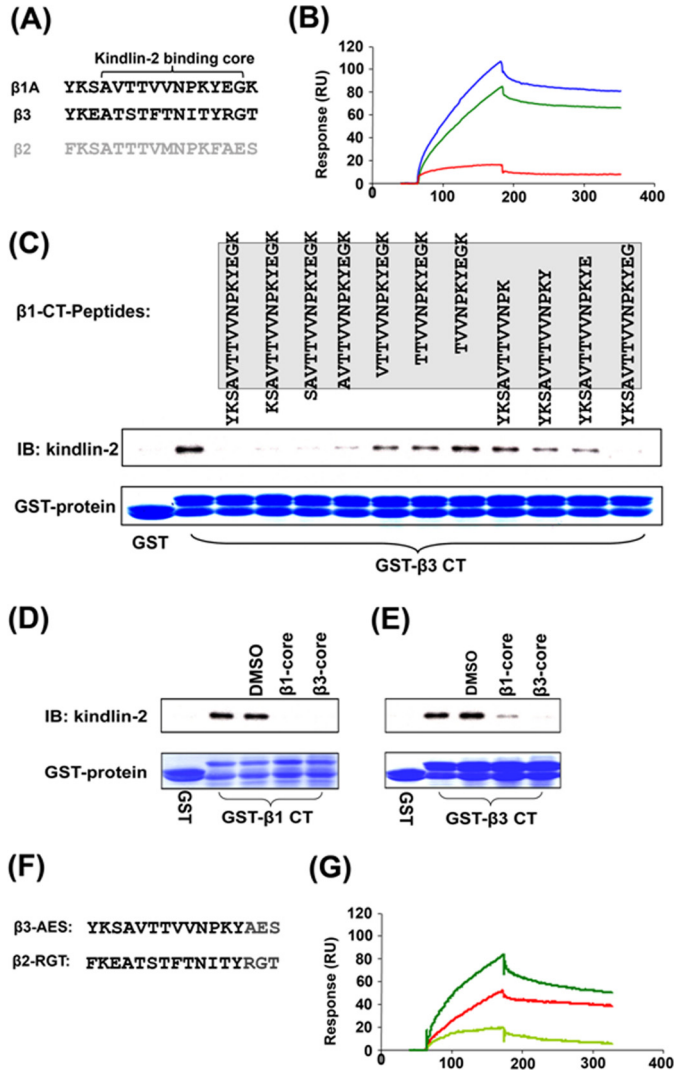

FIGURE 2. **Kindlin-2 interacts with the C termini of integrin β CTs.** *A*, amino acid sequences of the β_1, β_2, and β_3 C-terminal peptides. *B*, representative binding of one concentration (1 uM) of kindlin-2 to β C-terminal peptides. N-terminally biotinylated peptides were captured on a SA biosensor chip, and kindlin-2 binding signals were recorded after injection (*red* for β_2, *green* for β_3, and *blue* for β_1 peptides) as described in Fig. 1. *C*, control GST or GST-fused β_3 CT was incubated with HUVEC lysate in the presence of the indicated peptide from the β_1 CT (final concentration at 200 μM). The endogenous kindlin-2 binding to the β_3 CT was precipitated with glutathione-Sepharose and further analyzed by Western blot. GST-fused β1 CT (*D*) or GST-fused β3 CT (*E*) were used to precipitate kindlin-2 protein from HUVEC lysates in the presence of β1 core peptide or β3 core peptide as highlighted in *A*. *F*, the chimeric β_2 and β_3 CT with the last three-amino acid replacement. *G*, comparison of the binding of one concentration of kindlin-2 to N-terminally biotinylated β peptides (*light green* for β_3-AES, *red* for β_2-RGT, and *green* for the β_3 peptide as shown in *A*).

binding, and they play key roles in determining binding selectivity.

Kindlin-2-binding Core in Integrin β3 Cytoplasmic Tail Inhibits Cell Spreading—The functional significance of kindlin-2 binding core, β_3 (Ala^{750}–Gly^{761}), the β_3CT(CORE), was assessed in a cellular system. This segment, as well as control segments of the β_3 CT, was expressed as PSGL-1 chimera in CHO cell line stably expressing $\alpha_{IIb}\beta_3$ ($\alpha_{IIb}\beta_3$-CHO). The β_3 CT segments were expressed as fusion proteins linked to extracellular and transmembrane portions of PSGL-1 but with the β_3 CT replacing the PSGL-1 CT. As described previously (23), this strategy allows for intracellular expression of a selected β_3 CT segment, where it competes with the β_3 CT of the intact integrin and inhibits cell spreading on fibrinogen, a ligand for $\alpha_{IIb}\beta_3$, Monitoring of expression levels can be assessed in parallel with a PSGL-1 antibody. As assessed by flow cytometry, PSGL-1 expression differed by <10%, and the $\alpha_{IIb}\beta_3$ expression levels, monitored with a different antibody, were not affected by the transfections. Cell spreading was determined microscopically by measuring the surface area of 200 PSGL-1-expressing cells. Compared with cells expressing PSGL-1 alone, expression of the full-length β_3 CT fully inhibited cell spreading (Fig. 3). The β_3CT(CORE) expressing only the β_3 CT kindlin-2 binding core, β_3(749–762), was sufficient to significantly suppress cell spreading. The β_3CT(Δ748), which only expresses the talin but not the kindlin-2 binding site also significantly inhibited cell spreading (Fig. 3). These data are consistent with the contribution of both the talin-H and kindlin-2-binding domains in integrin-mediated functions and indicate that the kindlin-2-binding core itself plays an important regulatory role.

Kindlin-2 Is Unable to Directly Unclasp Integrin $\alpha_{IIb}\beta_3$ CT Complex—Unclasping the CT complex is the key step to induce the conformational change in the extracellular domain to trigger high affinity ligand recognition during the integrin activation (5, 16, 42). As a co-activator, we wanted to know whether kindlin-2 could directly unclasp the integrin CT complex. To test this possibility, NMR transferred NOE experiments were performed as we described previously to detect the integrin α/β CT clasp (16, 22). The transferred NOEs between α_{IIb} and MBP-β_3 were not reduced in the presence of kindlin-2 (Fig. 4*A*). In fact, the transferred NOEs are more pronounced in the presence of kindlin-2 indicating formation of a ternary complex involving α_{IIb}, MBP-β_3, and kindlin-2. This pattern contrasts with the dramatic reduction of the transferred NOEs observed for the α_{IIb}/MBP-β_3 in the presence of talin-H (Fig. 4*B*). These data indicate that kindlin-2 is unable to dissociate the integrin-cytoplasmic tails complex, which is consistent with the results of previous functional analyses showing that kindlin-2 enhanced talin-induced integrin activation but alone has only a minimal effect on integrin activation (23, 24).

Kindlin-2 and Talin Head Domain Can Bind Simultaneously to Integrin β_3 Cytoplasmic Tail—Because talin-H and kindlin-2 are capable of co-activating integrins by interaction with integrin β CT, it is conceivable that these two proteins might bind to one another or sterically influence the binding of each other to the β CT. To test these possibilities, we performed a series of SPR experiments. First, we considered whether talin-H and kindlin-2 could interact with each other. As shown in Fig. 5*A*, we failed to detect any binding signal when kindlin-2 protein at concentrations ranging from 87 nM to 700 nM was passed over immobilized talin-H. We verified that talin-H which had been immobilized on the biosensor chip was functional by its ability to bind the β_3 CT (data not shown). In addition, we failed to detect the binding of kindlin-2 to the talin-H subdomains including F_0F_1 and F_2F_3 (data not shown). As an independent approach, isothermal titration calorimetry experiments were performed and also showed no detectable interaction between kindlin-2 and talin-H with both constituents in solution (Fig. 5*B*). Thus, within the limits of sensitivity of SPR and isothermal

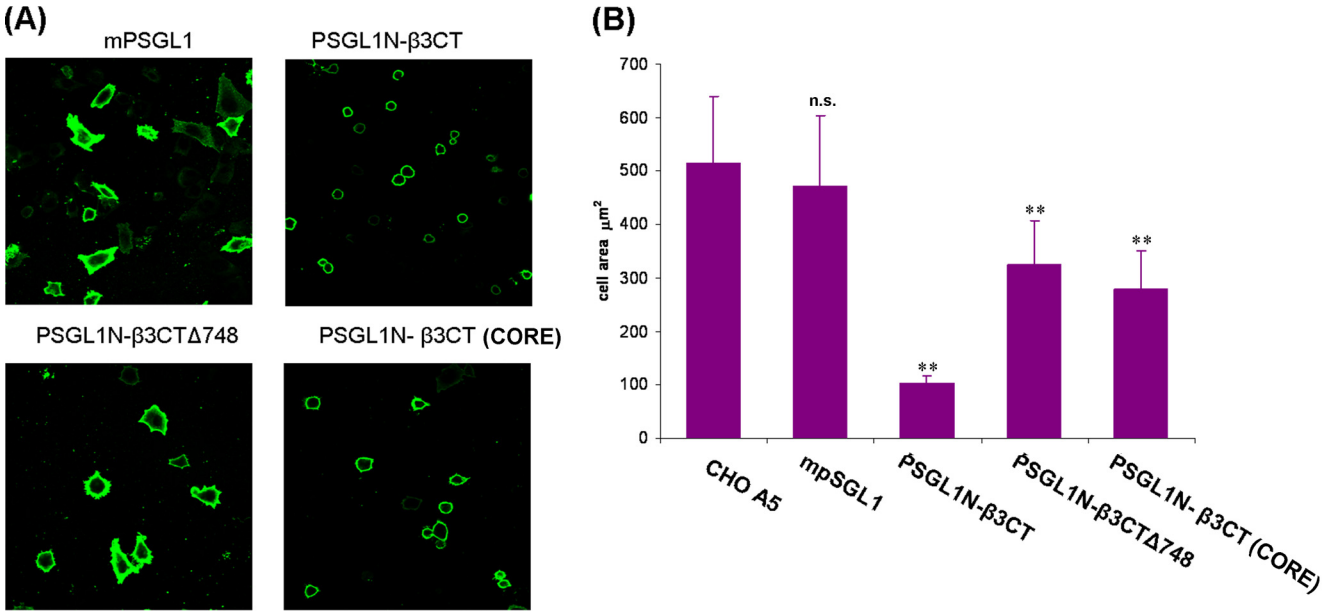

FIGURE 3. **The kindlin-2-binding core in the integrin β3 CT is sufficient to influence cell spreading.** CHO cells stabling expressing $\alpha_{IIb}\beta_3$ were transiently transfected with plasmids encoding the following β_3 CT-containing chimera: β_3CT/PSGL-1, β_3CTΔ748/PSGL-1, and β_3CT (CORE)/PSGL-1. The cells were allowed to adhere to fibrinogen coated coverslips 12 h after transfection, and cell spreading was measured after an additional 2 h. The adherent cells were fixed and stained with the anti-PSGL-1 mAb, KPL-1, for visualization of the expressing cells by fluorescence microscopy. *A* displays representative images taken at 40× (*bar*, 20 μm). *B* shows effects of the various chimera on integrin $\alpha_{IIb}\beta_3$-mediated cell spreading. The areas of PSGL-1-positive cells were measured using ImageJ software, and 200 cells were quantified in each experiment. The *error bars* represent means ± S.D. of three independent experiments. **, $p \leq 0.001$ *versus* CHO-A5 by Student's *t* test, *n.s.* indicates not significant ($p = 0.13$) *versus* CHO-A5 by *t* test.

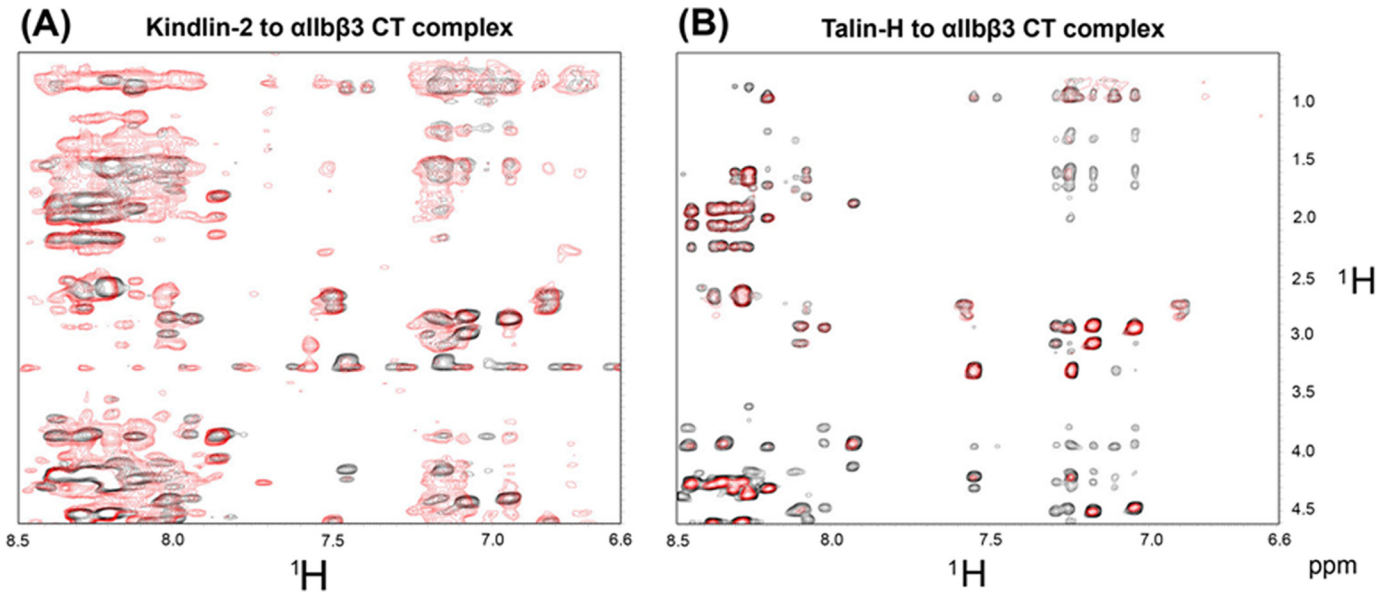

FIGURE 4. **Kindlin-2 fails to unclasp the integrin $\alpha_{IIb}\beta_3$ CT complex.** *A*, overlay of the selective region of transferred NOESY spectra of 2 mM α_{IIb} in the presence of 0.1 mM MBP-β_3 (*black*) *versus* 2 mM α_{IIb} in the presence of 0.1 mM MBP-β_3 and 0.2 mM kindlin-2 (*red*), showing that kindlin-2 does not disrupt the integrin $\alpha_{IIb}\beta_3$ CT complex formation. *B*, overlay of the selective region of transferred NOESY spectra of 2 mM α_{IIb} in the presence of 0.1 mM MBP-β_3 (*black*) *versus* 2 mM α_{IIb} in the presence of 0.1 mM MBP-β_3 and 0.05 mM talin-H (*red*), showing that talin-H disrupts the integrin $\alpha_{IIb}\beta_3$ CT complex.

titration calorimetry as performed, we could not detect interaction between talin-H and kindlin-2, although interaction of these proteins with β_3 CT indicates the functionality of the protein preparations.

The undetectable interaction between talin-H and kindlin-2 allowed us to test whether they can bind simultaneously to the integrin β CT by SPR experiments. Full-length β_3 CT was immobilized on the biosensor chip, and talin-H or kindlin-2 was passed over the chip. As shown in Fig. 6*A*, a typical progress curve was obtained for either kindlin-2 or talin-H. When a mixture of kindlin-2 and talin-H, each at the same concentration, was passed over the immobilized β_3 CT, the response curve was enhanced as compared with that obtained with each individual analyte, indicating that their interaction was not mutually exclusive (Fig. 6*A*). We further assessed whether occupancy of the immobilized β_3 CT with talin-H would limit kindlin-2 bind-

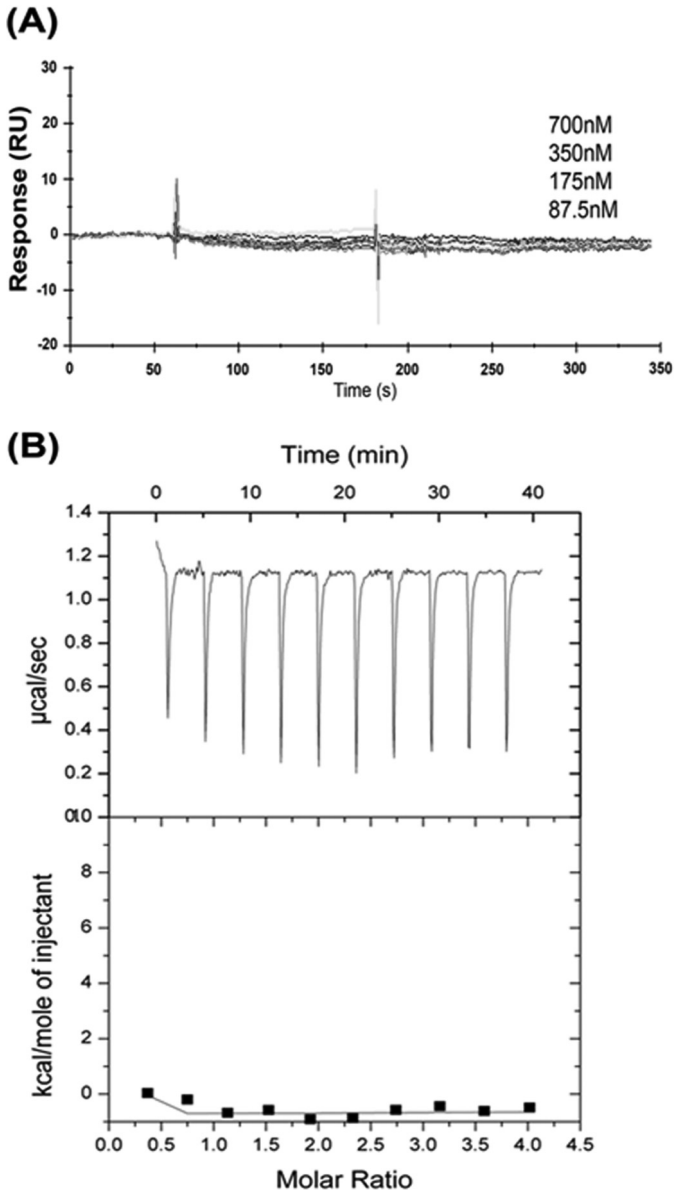

FIGURE 5. **Kindlin-2 and talin-H do not directly interact with each other.** *A*, SPR: talin-H was immobilized on the chip surfaces, and various concentrations of kindlin-2 protein were injected over the chip surface. The sensograms were collected on a Biacore3000 instrument. *B*, isothermal titration calorimetry: the *upper* plot represents the data obtained upon 3-μl injections of talin-H at 1.4 mM to 70 μM kindlin-2 solution. The *lower* graph shows the titration plot derived from the normalized integrated heats in kcal/mol of injectant plotted against molar ratio after background subtraction. There is no significant difference in the heat changes between different injections of talin-H indicative of no direct interaction of kindlin-2 to talin-H.

ing. As shown in Fig. 6*B*, after the β_3 CT-coated chip was saturated with talin-H, the binding signal induced by kindlin-2 reached the level observed in the absence of talin-H. Furthermore, we measured the binding pattern of talin-H to immobilized β_3 CT by sequential injections (500-s intervals) in the presence or absence of kindlin-2. The binding signals obtained with multiple injections of talin-H onto immobilized β_3 CT was unaffected by kindlin-2 in the running buffer (Fig. 6, *C* and *D*). The same results were obtained when we used β_1 CT instead of β_3 CT in these experiments. Together, these data support the conclusion that talin-H and kindlin-2 can interact simultaneously with integrin β CTs and exert minimal effects on the binding of one another to the β CT.

To provide independent evidence for the ability of talin-H, kindlin-2, and β_3 CT to form a ternary complex, we again used a NMR approach. As shown in Fig. 7*A*, when talin-F_2F_3 interacts with ^{15}N-labeled β_3 CT, significant line-broadening or chemical shift changes occur, indicative of complex formation. Similarly, line-broadening and chemical shift changes were also noted when kindlin-2 was added to the ^{15}N-labeled β_3 CT (Fig. 7*B*). If kindlin-2 and talin-F_2F_3 were to compete with each other, the spectrum of ^{15}N-labeled β_3 CT mixed with both talin-F_2F_3 and kindlin-2 would overlay with or mimic one of the single binding partners. As an example, the chemical shifts induced by filamin binding to the β_3 CT are neutralized by addition of migfilin (8). However, when talin-F_2F_3 and kindlin-2 were added to the β_3 CT, further line-broadening and spectral changes were observed (Fig. 7*C*), indicative of distinct perturbations reflecting formation of a ternary complex. Thus, both SPR and NMR experiments support the formation of a ternary complex involving talin, kindin-2, and the β_3 CT.

DISCUSSION

Kindlin family members were recently identified as integrin co-activators that play indispensable roles in integrin activation (43). Our current study reports several novel findings to further interpret the mechanism by which kindlin-2 facilitates integrin activation. First, kindlin-2 shows selectivity in binding to integrin CT; it binds with substantially lower affinity to β_2 than to β_1 and β_3 CT. β_2-integrins also require kindlins for activation, and this need may be met by kindlin-3 in myeloid cells (27–29). Second, the kindlin-2 binding core of 12 amino acids has been identified in integrin β CTs, which includes the conserved membrane-distal N*xx*Y region and S/T cluster as well as the variable residues flanking these two motifs. The functional importance of this kindlin-2 binding core in intact cells was supported by cell spreading assays. Expression of the C-terminal kindlin-2 binding region alone was sufficient to suppress integrin mediated cell spreading. The identification of the kindlin-2 binding core provides a context in which to interpret the effects of previously reported mutations on integrin activation. Thus, the effects of $\beta_3\Delta755$, as well single point mutations at S752P or Y759A in the β_3CT on integrin activation (44–49) can be attributed to inhibition of kindlin-2 binding. Also, the inhibition of integrin $\alpha_{IIb}\beta_3$ activation in platelets by importable peptides corresponding to β_3(743–750) and β_3(749–756), which overlap the kindlin-2 binding core (50, 51), can now be attributed to effects on kindlin binding. Expression of the β_3CTΔ748 and β_3CT (CORE) as a PSGL chimeric protein also suppressed integrin activation, suggesting that the membrane proximal and membrane distal regions of the β_3CT contribute independently to integrin-mediated responses, observations consistent with the cooperativity between talin and kindlin-2 in integrin function. We cannot exclude that the effects of these two regions may also reflect their interaction with other integrin binding partners. For example, Integrin Linked Kinase (52) and Src

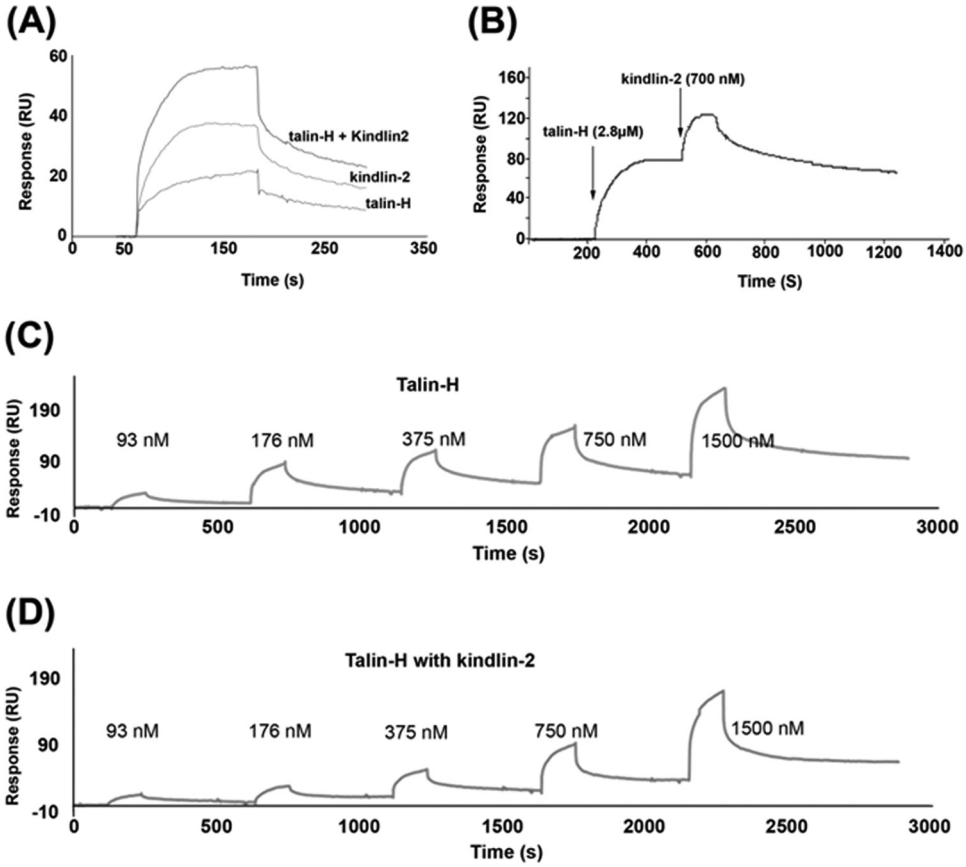

FIGURE 6. **Kindlin-2 and talin head domain can associate simultaneously with the integrin β_3 CT.** *A*, kindlin-2, talin-H, or their mixture, at the same individual concentrations (700 nM), was injected over the sensor chips coated with full-length β_3 CT, and their association properties were recorded. *B*, the β_3 CT coated sensor chip was first saturated with a high concentration (2.8 μM) of talin-H. Once the binding reached the maximal level, kindlin-2 (700 nM) was injected. Increasing concentrations of talin-H were injected over sensor chips coated with full-length β_3 CT with (*C*) or without (*D*) kindlin-2 in running buffer.

(53) have been shown to bind to the C-terminal region of the β_3 CT as well. However, in the $\alpha_{IIb}\beta_3$-CHO cell system, these specific binding partners do not influence $\alpha_{IIb}\beta_3$ activation or co-activation with talin-H (54).[4]

Instead of N*xx*Y in β_1 and β_3 tails, the counterpart motif in the β_2 CT is N*xx*F. However, substitution of Phe with Tyr in β_2 CT did not improve the binding affinity (data not shown), suggesting that the non-conserved residues in the integrin β core region might be also critical for kindlin-2 recognition. This proposition was supported experimentally. A β_2 CT peptide with its C-terminal AES replaced by the β_3 RGT showed higher kindlin-2 binding, and conversely, a β_3 CT peptide in which it C-terminal RGT was replaced with the β_2 AES sequence had blunted kindlin-2 binding (Fig. 2). Even though this binding core is sufficient for kindlin-2 binding to β_1 and β_3 CT, we do not exclude the possibility that more membrane proximal residues in the CT might help to stabilize the interaction and support integrin activation. More detailed structural studies are still required to further understand the binding specificity of the kindlin/βCT interaction. Third, kindlin-2 is unable to directly unclasp the integrin CT complex, which provides a mechanistic explanation for the very limited ability of kindlin-2 alone on integrin activation; for efficient activation, talin-H also has to be present (23, 24). One possibility for the talin/kindlin-2 co-activating requirement is that talin-H might directly interact with kindlin-2. However, we failed to detect their direct interaction experimentally. Indeed, talin-H and kindlin-2 can bind simultaneously to integrin β CT with no evidence of mutual perturbation. The capacity of kindlin-2 and talin-H to co-assemble on the β_3 CT to form a ternary complex was indicated by our SPR data, where the resonance unit signal, a reflection of mass of the bound constituents (55, 56) increased upon binding of both talin-H and kindlin-2 to the immobilized β_3 CT. Independent evidence of formation of a ternary complex also was provided by NMR experiments showing that the chemical shifts induced by talin-H or kindlin-2 binding to the β_3 CT were further shifted by the presence of the two constituents; such changes are also indicative of simultaneous interaction of the three constituents, *i.e.* formation of a ternary complex. Of note, the ability to detect chemical shift changes in the β_3 CT upon addition of kindlin-2 suggests that it may be feasible to locate the interactive residues in β_3 CT engaged in kindlin-2 binding. In view of the relatively low affinity of kindlin-2 for the β_3 CT, which we estimated from our SPR experiments to be 1.36×10^{-7} M, such NMR mapping may be more

[4] K. Bledzka, J. Liu, Z. Xu, H. D. Perera, S. P. Yadav, K. Bialkowska, J. Qin, Y.-Q. Ma, and E. F. Plow, unpublished observations.

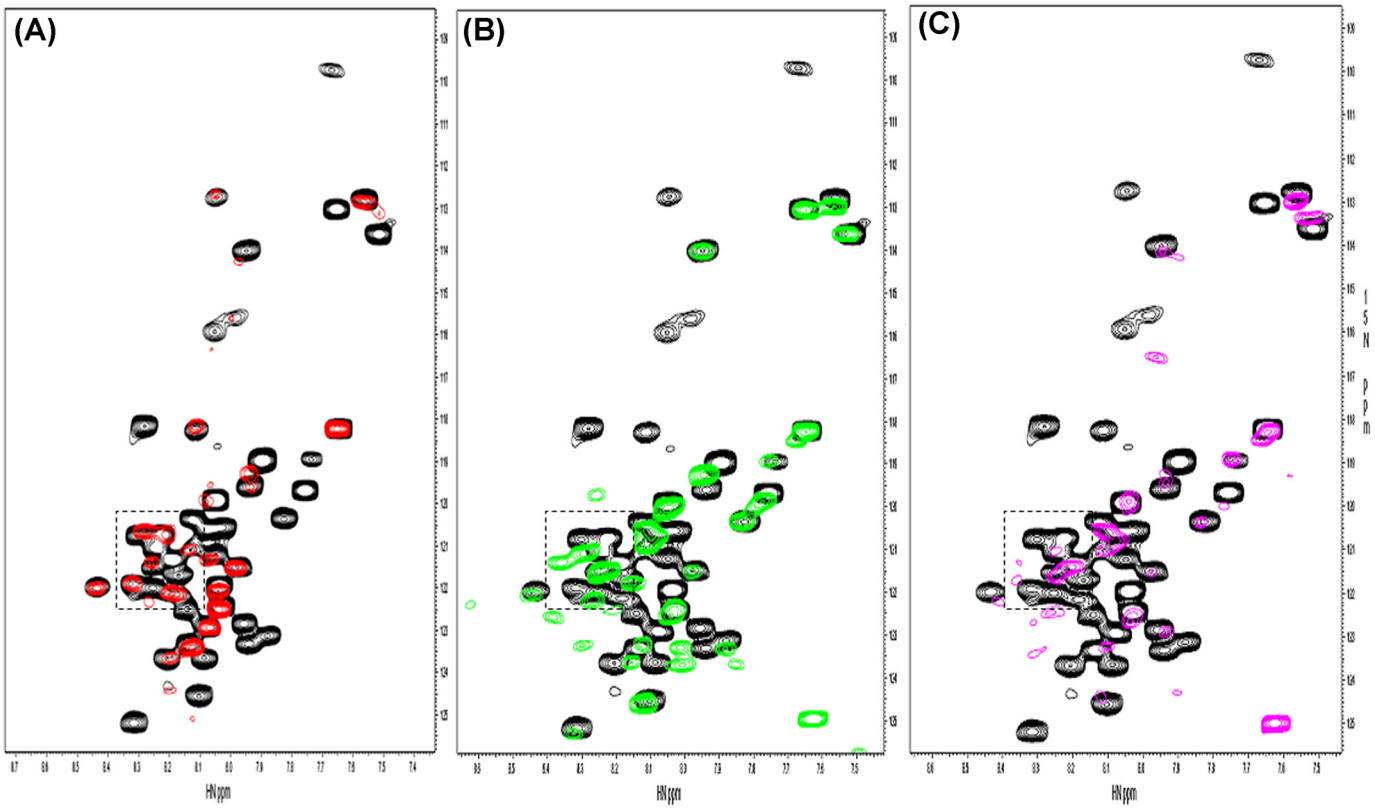

FIGURE 7. *A*, demonstration of a ternary complex between kindlin-2, β_3CT, and talin by NMR. ^{15}N-labeled HSQC of β_3 CT (60 μM) in the absence (*black*) and presence (*red*) of unlabeled talin-F_2F_3 (100 μM), pH 6.1. Significant line-broadening and some chemical shift changes occur upon addition of talin-F_2F_3 to the ^{15}N-labeled β_3 CT (*B*). ^{15}N-labeled HSQC of β_3CT (60 μM) in the absence (*black*) and presence (*green*) of unlabeled kindlin-2 (100 μM), pH 6.1. The pattern of line-broadening and chemical shift changes differ from that of *A* by talin-F_2F_3, indicating a different binding mode. *C*, ^{15}N-labeled HSQC of β_3CT (60 μM) in the absence (*black*) and presence (*cyan*) of talin-F_2F_3 (100 μM) and kindlin-2 (100 μM), pH 6.1. More line broadening and chemical shift changes occur with some new peaks, which differ from *A* and *B*, indicating formation of a ternary complex.

feasible for detecting and dissecting the ternary complex than other approaches that are difficult to apply for lower affinity interactions. However, because of the relatively large molecular weight involving kindlin-2 (~70 kDa) and talin-H (~50 kDa), future investigation will employ deuteration and transverse relaxation optimized spectroscopy-type NMR experiments to reduce the line-broadening effect (57). Although we did not detect any synergistic binding effect of kindlin-2 and talin-H on integrin β CT, their simultaneous binding might be the first key step to attain synergy in integrin activation through alternative pathways: i) kindlin-2 and talin-H could jointly displace negative regulator(s) such as filamin from the integrin CTs. The site that we have mapped for kindlin-2 binding on integrin CT clearly overlaps with that identified for filamin (7); ii) kindlin-2 and talin might be linked by an as yet identified bridging molecule(s), thereby enhancing their interaction with integrin; iii) more directly, kindlin-2 could attach onto the plasma membrane and place β CT in a specific orientation advantageous for talin-H recognition. Although these possible regulatory mechanisms remain to be vigorously dissected, our studies herein have provided significant insights into our understanding of how kindlin-2 and talin may be simultaneously situated on integrin β CT and synergistically promote integrin activation. The capacity of talin and kindlins to associate simultaneously provides an example as to how large molecules such as talin and kindlins can associate in close proximity on a small segment of receptor, the β CTs, to orchestrate a physiologically relevant cellular response, integrin activation.

REFERENCES

1. Hynes, R. O. (2002) Integrins: Bidirectional, allosteric signaling machines. *Cell* **110,** 673–687
2. Luo, B. H., Carman, C. V., and Springer, T. A. (2007) Structural basis of integrin regulation and signaling. *Annu. Rev. Immunol.* **25,** 619–647
3. Yang, J., Ma, Y. Q., Page, R. C., Misra, S., Plow, E. F., and Qin, J. (2009) Structure of an integrin $\alpha_{IIb}\beta_3$ transmembrane-cytoplasmic heterocomplex provides insight into integrin activation. *Proc. Natl. Acad. Sci. U.S.A.* **106,** 17729–17734
4. Lau, T. L., Kim, C., Ginsberg, M. H., and Ulmer, T. S. (2009) The structure of the integrin $\alpha_{IIb}\beta_3$ transmembrane complex explains integrin transmembrane signaling. *EMBO J.* **28,** 1351–1361
5. Qin, J., Vinogradova, O., and Plow, E. F. (2004) Integrin bidirectional signaling: A molecular view. *PLoS. Biol.* **2,** e169
6. Ma, Y. Q., Qin, J., and Plow, E. F. (2007) Platelet integrin $\alpha_{IIb}\beta_3$: Activation mechanisms. *J. Thromb. Haemost.* **5,** 1345–1352
7. Kiema, T., Lad, Y., Jiang, P., Oxley, C. L., Baldassarre, M., Wegener, K. L., Campbell, I. D., Ylänne, J., and Calderwood, D. A. (2006) The molecular basis of filamin binding to integrins and competition with talin. *Mol. Cell* **21,** 337–347
8. Ithychanda, S. S., Das, M., Ma, Y. Q., Ding, K., Wang, X., Gupta, S., Wu, C., Plow, E. F., and Qin, J. (2009) Migfilin, a molecular switch in regulation of integrin activation. *J. Biol. Chem.* **284,** 4713–4722
9. Anthis, N. J., Haling, J. R., Oxley, C. L., Memo, M., Wegener, K. L., Lim, C. J., Ginsberg, M. H., and Campbell, I. D. (2009) β Integrin tyrosine phosphorylation is a conserved mechanism for regulating talin-induced integrin activation. *J. Biol. Chem.* **284,** 36700–36710

10. Bledzka, K., Bialkowska, K., Nie, H., Qin, J., Byzova, T., Wu, C., Plow, E. F., and Ma, Y. Q. (2010) Tyrosine phosphorylation of integrin β3 regulates kindlin-2 binding and integrin activation. *J. Biol. Chem.* **285,** 30370–30374
11. Hoyer, D., and Boddeke, H. W. (1993) Partial agonists, full agonists, antagonists: Dilemmas of definition. *Trends Pharmacol. Sci.* **14,** 270–275
12. Calderwood, D. A. (2004) Talin controls integrin activation. *Biochem. Soc. Trans.* **32,** 434–437
13. Campbell, I. D., and Ginsberg, M. H. (2004) The talin-tail interaction places integrin activation on FERM ground. *Trends Biochem. Sci.* **29,** 429–435
14. Calderwood, D. A., Zent, R., Grant, R., Rees, D. J., Hynes, R. O., and Ginsberg, M. H. (1999) The Talin head domain binds to integrin β subunit cytoplasmic tails and regulates integrin activation. *J. Biol. Chem.* **274,** 28071–28074
15. Yan, B., Calderwood, D. A., Yaspan, B., and Ginsberg, M. H. (2001) Calpain cleavage promotes talin binding to the β3 integrin cytoplasmic domain. *J. Biol. Chem.* **276,** 28164–28170
16. Vinogradova, O., Velyvis, A., Velyviene, A., Hu, B., Haas, T., Plow, E., and Qin, J. (2002) A structural mechanism of integrin $\alpha_{IIb}\beta_3$ "inside-out" activation as regulated by its cytoplasmic face. *Cell* **110,** 587–597
17. García-Alvarez, B., de Pereda, J. M., Calderwood, D. A., Ulmer, T. S., Critchley, D., Campbell, I. D., Ginsberg, M. H., and Liddington, R. C. (2003) Structural determinants of integrin recognition by talin. *Mol. Cell* **11,** 49–58
18. Tadokoro, S., Shattil, S. J., Eto, K., Tai, V., Liddington, R. C., de Pereda, J. M., Ginsberg, M. H., and Calderwood, D. A. (2003) Talin binding to integrin β tails: A final common step in integrin activation. *Science* **302,** 103–106
19. Vinogradova, O., Vaynberg, J., Kong, X., Haas, T. A., Plow, E. F., and Qin, J. (2004) Membrane-mediated structural transitions at the cytoplasmic face during integrin activation. *Proc. Natl. Acad. Sci. U.S.A.* **101,** 4094–4099
20. Han, J., Lim, C. J., Watanabe, N., Soriani, A., Ratnikov, B., Calderwood, D. A., Puzon-McLaughlin, W., Lafuente, E. M., Boussiotis, V. A., Shattil, S. J., and Ginsberg, M. H. (2006) Reconstructing and deconstructing agonist-induced activation of integrin $\alpha_{IIb}\beta_3$. *Curr. Biol.* **16,** 1796–1806
21. Wegener, K. L., Partridge, A. W., Han, J., Pickford, A. R., Liddington, R. C., Ginsberg, M. H., and Campbell, I. D. (2007) Structural basis of integrin activation by talin. *Cell* **128,** 171–182
22. Ma, Y. Q., Yang, J., Pesho, M. M., Vinogradova, O., Qin, J., and Plow, E. F. (2006) Regulation of integrin $\alpha_{IIb}\beta_3$ activation by distinct regions of its cytoplasmic tails. *Biochemistry* **45,** 6656–6662
23. Ma, Y. Q., Qin, J., Wu, C., and Plow, E. F. (2008) Kindlin-2 (Mig-2): A co-activator of β3 integrins. *J. Cell Biol.* **181,** 439–446
24. Montanez, E., Ussar, S., Schifferer, M., Bösl, M., Zent, R., Moser, M., and Fässler, R. (2008) Kindlin-2 controls bidirectional signaling of integrins. *Genes Dev.* **22,** 1325–1330
25. Harburger, D. S., Bouaouina, M., and Calderwood, D. A. (2009) Kindlin-1 and -2 directly bind the C-terminal region of β integrin cytoplasmic tails and exert integrin-specific activation effects. *J. Biol. Chem.* **284,** 11485–11497
26. Ussar, S., Moser, M., Widmaier, M., Rognoni, E., Harrer, C., Genzel-Boroviczeny, O., and Fässler, R. (2008) Loss of Kindlin-1 causes skin atrophy and lethal neonatal intestinal epithelial dysfunction. *PLoS. Genet.* **4,** e1000289
27. Malinin, N. L., Zhang, L., Choi, J., Ciocea, A., Razorenova, O., Ma, Y. Q., Podrez, E. A., Tosi, M., Lennon, D. P., Caplan, A. I., Shurin, S. B., Plow, E. F., and Byzova, T. V. (2009) A point mutation in KINDLIN3 ablates activation of three integrin subfamilies in humans. *Nat. Med.* **15,** 313–318
28. Moser, M., Bauer, M., Schmid, S., Ruppert, R., Schmidt, S., Sixt, M., Wang, H. V., Sperandio, M., and Fässler, R. (2009) Kindlin-3 is required for β2 integrin-mediated leukocyte adhesion to endothelial cells. *Nat. Med.* **15,** 300–305
29. Svensson, L., Howarth, K., McDowall, A., Patzak, I., Evans, R., Ussar, S., Moser, M., Metin, A., Fried, M., Tomlinson, I., and Hogg, N. (2009) Leukocyte adhesion deficiency-III is caused by mutations in KINDLIN3 affecting integrin activation. *Nat. Med.* **15,** 306–312
30. Ussar, S., Wang, H. V., Linder, S., Fässler, R., and Moser, M. (2006) The Kindlins: subcellular localization and expression during murine development. *Exp. Cell Res.* **312,** 3142–3151
31. Tu, Y., Wu, S., Shi, X., Chen, K., and Wu, C. (2003) Migfilin and Mig-2 link focal adhesions to filamin and the actin cytoskeleton and function in cell shape modulation. *Cell* **113,** 37–47
32. Perera, H. D., Ma, Y. Q., Yang, J., Hirbawi, J., Plow, E. F., and Qin, J. (2011) Membrane binding of the N-terminal ubiquitin-like domain of kindlin-2 is crucial for its regulation of integrin activation. *Structure* **19,** 1664–1671
33. Liu, J., Fukuda, K., Xu, Z., Ma Y. Q., Hirbawi, J., Mao, X., Wu, C., Plow E. F., and Qin, J. (2011) Structural basis of phosphoinositide binding to kindlin-2 protein pleckstrin homology domain in regulating integrin activation. *J. Biol. Chem.* **286,** 43334–43342
34. Qu, H., Tu, Y., Shi, X., Larjava, H., Saleem, M. A., Shattil, S. J., Fukuda, K., Qin, J., Kretzler, M., and Wu, C. (2011) Kindlin-2 regulates podocyte adhesion and fibronectin matrix deposition through interactions with phosphoinositides and integrins. *J. Cell Sci.* **124,** 879–891
35. Shi, X., Ma, Y. Q., Tu, Y., Chen, K., Wu, S., Fukuda, K., Qin, J., Plow, E. F., and Wu, C. (2007) The MIG-2/integrin interaction strengthens cell-matrix adhesion and modulates cell motility. *J. Biol. Chem.* **282,** 20455–20466
36. Moser, M., Nieswandt, B., Ussar, S., Pozgajova, M., and Fässler, R. (2008) Kindlin-3 is essential for integrin activation and platelet aggregation. *Nat. Med.* **14,** 325–330
37. Plow, E. F., and Shattil, S. J. (2001) Integrin $\alpha_{IIb}\beta_3$ and platelet aggregation in *Hemostasis and Thrombosis: Basic Principles and Clinical Practice* (Colman, R. W., Hirsh, J., Marder, V. J., Clowes, A. W., and George, J. N., eds) pp. 479–491, Lippincott Williams & Wilkins, Philadelphia, PA
38. Shimaoka, M., Takagi, J., and Springer, T. A. (2002) Conformational regulation of integrin structure and function. *Annu. Rev. Biophys. Biomol. Struct.* **31,** 485–516
39. Hood, J. D., and Cheresh, D. A. (2002) Role of integrins in cell invasion and migration. *Nat. Rev. Cancer* **2,** 91–100
40. Goksoy, E., Ma, Y. Q., Wang, X., Kong, X., Perera, D., Plow, E. F., and Qin, J. (2008) Structural basis for the autoinhibition of talin in regulating integrin activation. *Mol. Cell* **31,** 124–133
41. Delaglio, F., Grzesiek, S., Vuister, G. W., Zhu, G., Pfeifer, J., and Bax, A. (1995) NMRPipe: A multidimensional spectral processing system based on UNIX pipes. *J. Biomol. NMR* **6,** 277–293
42. Hughes, P. E., Diaz-Gonzalez, F., Leong, L., Wu, C., McDonald, J. A., Shattil, S. J., and Ginsberg, M. H. (1996) Breaking the integrin hinge. A defined structural constraint regulates integrin signaling. *J. Biol. Chem.* **271,** 6571–6574
43. Malinin, N. L., Plow E. F., and Byzova, T. V. (2010) Kindlins in FERM adhesion. *Blood* **115,** 4011–4017
44. Chen, Y. P., Djaffar, I., Pidard, D., Steiner, B., Cieutat, A. M., Caen, J. P., and Rosa, J. P. (1992) Ser-752→Pro mutation in the cytoplasmic domain of integrin β3 subunit and defective activation of platelet integrin $\alpha_{IIb}\beta_3$ (glycoprotein IIb-IIIa) in a variant of Glanzmann thrombasthenia. *Proc. Natl. Acad. Sci. U.S.A.* **89,** 10169–10173
45. Chen, Y. P., O'Toole, T. E., Ylänne, J., Rosa, J. P., and Ginsberg, M. H. (1994) A point mutation in the integrin β3 cytoplasmic domain (Ser-752→Pro) impairs bidirectional signaling through $\alpha_{IIb}\beta_3$ (platelet glycoprotein IIb-IIIa). *Blood* **84,** 1857–1865
46. Hughes, P. E., O'Toole, T. E., Ylänne, J., Shattil, S. J., and Ginsberg, M. H. (1995) The conserved membrane-proximal region of an integrin cytoplasmic domain specifies ligand binding affinity. *J. Biol. Chem.* **270,** 12411–12417
47. Schaffner-Reckinger, E., Gouon, V., Melchior, C., Plançon, S., and Kieffer, N. (1998) Distinct involvement of beta3 integrin cytoplasmic domain tyrosine residues 747 and 759 in integrin-mediated cytoskeletal assembly and phosphotyrosine signaling. *J. Biol. Chem.* **273,** 12623–12632
48. Xi, X., Bodnar, R. J., Li, Z., Lam, S. C., and Du, X. (2003) Critical roles for the COOH-terminal NITY and RGT sequences of the integrin β3 cytoplasmic domain in inside-out and outside-in signaling. *J. Cell Biol.* **162,** 329–339
49. Zou, Z., Chen, H., Schmaier, A. A., Hynes, R. O., and Kahn, M. L. (2007)

Structure-function analysis reveals discrete β3 integrin inside-out and outside-in signaling pathways in platelets. *Blood* **109,** 3284–3290
50. Hers, I., Donath, J., Litjens, P. E., van Willigen, G., and Akkerman, J. W. (2000) Inhibition of platelet integrin $\alpha_{IIb}\beta_3$ by peptides that interfere with protein kinases and the β3 tail. *Arterioscler. Thromb. Vasc. Biol.* **20,** 1651–1660
51. Dimitriou, A. A., Stathopoulos, P., Mitsios, J. V., Sakarellos-Daitsiotis, M., Goudevenos, J., Tsikaris, V., and Tselepis, A. D. (2009) Inhibition of platelet activation by peptide analogs of the β3-intracellular domain of platelet integrin $\alpha_{IIb}\beta_3$ conjugated to the cell-penetrating peptide Tat(48–60). *Platelets* **20,** 539–547
52. Hannigan, G. E., Leung-Hagesteijn, C., Fitz-Gibbon, L., Coppolino, M. G., Radeva, G., Filmus, J., Bell, J. C., and Dedhar, S. (1996) Regulation of cell adhesion and anchorage-dependent growth by a new β1-integrin-linked protein kinase. *Nature* **379,** 91–96
53. Obergfell, A., Eto, K., Mocsai, A., Buensuceso, C., Moores, S. L., Brugge, J. S., Lowell, C. A., and Shattil, S. J. (2002) Coordinate interactions of Csk, Src, and Syk kinases with $\alpha_{IIb}\beta_3$ initiate integrin signaling to the cytoskeleton. *J. Cell Biol.* **157,** 265–275
54. Legate, K. R., and Fässler, R. (2009) Mechanisms that regulate adaptor binding to β-integrin cytoplasmic tails. *J. Cell Sci.* **122,** 187–198
55. Stenberg E., Persson B., Roos H., Urbaniczky C., (1991) *J. Colloid Interface Sci.* **143,** 513–526
56. Kodoyianni, V. (2011) Label-free analysis of biomolecular interactions using SPR imaging. *BioTechniques* **50,** 32–40
57. Vinogradova, O., and Qin, J. (2012) NMR as a unique tool in assessment and complex determination of weak protein-protein interactions. *Top. Curr. Chem.* **326,** 35–45